

## CPPD and Associated Crystals in Clinically Diagnosed Chondrocalcinosis: A Clinicopathological Study of 20 Patients

Ágnes Apáthy<sup>1</sup> and Miklós Bély<sup>2\*</sup>

### Abstract

**Introduction:** Chondrocalcinosis (Ch-C), induced by calcium pyrophosphate dihydrate crystals (CPPD)  $[Ca_2P_2O_7 \cdot 2H_2O]$  is considered as a distinct metabolic disease and a well-defined clinical entity, with characteristic clinical manifestations and symptoms. This study used previously found method by the author .i.e, non-staining approach to discover crystal deposits in patients with clinically diagnosed Ch-C, to find a possible correlation between coexisting crystals, and to assess the role of coexistent crystals in inflammatory cellular processes of joints.

**Patients and methods:** There were forty (40) surgical specimens that had been traditionally processed from 16 patients who had been clinically diagnosed with Ch-C.

**Results:** In unstained tissue sections CPPD crystals were found in 22 of 40 samples of all 16 patients. Beside the CPPD crystals calcium hydroxyapatite (HA)  $[Ca_5(PO_4)_3(OH)]$  crystals were found in 26 tissue samples of all 16 patients, cholesterol (CC)  $[C_{27}H_{46}O]$  in 23 tissue samples of 12 patients, and crystalline liquid lipid droplets (CL) in 11 tissue samples of 5 patients. More or less amorphous deposits of calcium carbonate  $[CaCO_3]$  and/or calcium phosphate  $[Ca_3(PO_4)_2]$  were present alongside CPPD and the contemporaneous crystals. There was a significant and positive correlation between prevalence of CPPD and HA. The connection between inflammatory cellular infiltration and CPPD, HA, CC or CL crystals surrounded by mineral deposits was not significant.

**Conclusions:** The non-staining approach is a practical, low-tech way to find CPPD, HA, CC, and other crystals (with or without CL). The positive and significant correlation between CPPD and HA support the earlier premise that CPPD and HA represent basically an identical metabolic disorder). CPPD and/or HA crystals can provoke inflammatory processes responsible for the clinical symptoms, but the variable amounts

<sup>1</sup>Department of Rheumatology, St. Margaret Clinic, Budapest, Hungary

<sup>2</sup>Department of Pathology, Hospital of the Order of the Brothers of Saint John of God in Budapest, Hungary

\*Corresponding Author: Miklós Bély, Department of Pathology, Hospital of the Order of the Brothers of Saint John of God in Budapest, Hungary.

Received Date: 02-09-2024

Accepted Date: 02-17-2024

Published Date: 02-29-2024

Copyright© 2024 by Apáthy A, et al. All rights reserved. This is an open-access article distributed under the terms of the Creative Commons Attribution License, which permits unrestricted use, distribution, and reproduction in any medium, provided the original author and source are credited.

of amorphous minerals enclose (isolate) the crystals, and can reduce or eliminate the inflammatory reaction. The authors assume that CC (with or without CL) is an associated phenomenon (concomitant fat metabolic malady) without direct cause of inflammation, and is not responsible for clinical symptoms of crystal induced arthropathies.

**Keywords:** Chondrocalcinosis; Nonstaining technique, Coexisting crystals; Inflammatory processes.

**Abbreviations:** Ch-C: Chondrocalcinosis; AR: Apatite Rheumatism; CPPD: Calcium Pyrophosphate Dehydrate  $[\text{Ca}_2\text{P}_2\text{O}_7 \cdot 2\text{H}_2\text{O}]$ ; HA: Calcium Hydroxyapatite  $[\text{Ca}_5(\text{PO}_4)_3(\text{OH})]$ ; CC: Cholesterol Crystals  $[\text{C}_{27}\text{H}_{46}\text{O}]$ ; CL: Crystalline LIQUID LIPID Spherules; MSU: Monosodium Urate Monohydrate  $[\text{NaC}_5\text{H}_3\text{N}_4\text{O}_3 \cdot \text{H}_2\text{O}]$ ; Crystal: Crystalline Monosodium Salt of Uric Acid  $[\text{C}_5\text{H}_4\text{N}_4\text{O}_3]$ ; HE: Hematoxylin Eosin; Ts: Tissue Samples.

## Introduction

Chondrocalcinosis, pseudogout, and pyrophosphate arthropathy are examples of arthritic conditions brought on by calcium pyrophosphate dihydrate  $[\text{Ca}_2\text{P}_2\text{O}_7 \cdot 2\text{H}_2\text{O}]$  crystals, considered as a distinct metabolic disease and a well-defined clinical entity, with characteristic clinical manifestations and symptoms [1-8].

The CPPD crystals exhibit a moderate subchronic-chronic inflammatory infiltration of lymphoplasmacytes and macrophages (giant cells), or that are characterized by fibrosis with nearly complete absence of inflammatory reaction. Typically, the crystals are accompanied by amorphous calcium phosphate  $[\text{Ca}_3(\text{PO}_4)_2]$  and/or calcium carbonate  $[\text{CaCO}_3]$  deposition. In surgical pathology, "non-staining" procedures were first introduced by Bély M, et al. [9], which ushered in a new age for crystal diagnostics and the identification of crystals other than CPPD in cases of chondrocalcinosis and other metabolic illnesses [9]. This innovative, delicate technique works well to pinpoint the CPPD, calcium hydroxyapatite (HA)  $[\text{Ca}_5(\text{PO}_4)_3(\text{OH})]$ , monosodium urate monohydrate (MSU)  $[\text{NaC}_5\text{H}_3\text{N}_4\text{O}_3 \cdot \text{H}_2\text{O}]$ -

monosodium salt of uric acid  $[\text{C}_5\text{H}_4\text{N}_4\text{O}_3]$ , cholesterol (CC)  $[\text{C}_{27}\text{H}_{46}\text{O}]$  crystals, crystalline liquid lipid droplets (CL), furthermore, to recognize (distinguish, discover) other morphologically not identified crystals in paraffin embedded, unstained, formalin-fixed tissue sections observed under polarized light [9-15].

The objectives of this study were to:

- Use the Bély M, et al. [9], non-staining technique to identify crystal deposits in patients with clinically diagnosed chondrocalcinosis
- Compare the non-staining technique's efficacy with that of conventional HE stains
- Characterize the primary characteristics of concurrent crystals.
- To find a possible correlation between coexisting crystals, and
- To assess the role of coexistent crystals in inflammatory cellular processes of joints.

## Patients and methods

Sixteen (16) joints (knee n=8, hip n=4, wrist n=2, elbow n=1, shoulder n=1) of 16 patients with clinically diagnosed Ch-C were operated;

40 surgical specimens were available (synovial membrane n=15, capsule n=15, bone and/or cartilage n=5, bursa n=3, tendon n=2). After being fixed for at least 24 hours at room temperature (20 Co) in an 8% aqueous solution of formaldehyde [CH<sub>2</sub>(OH)<sub>2</sub>] at pH 7.6, the tissue samples were embedded in paraffin. Five micron deparaffinized serial sections were stained with HE [16], Alizarin red S (calcium-specific staining) [17,18], or von Kossa's reaction (phosphate [Ca<sub>3</sub>(PO<sub>4</sub>)<sub>2</sub>] and/or carbonate [CaCO<sub>3</sub>]) [17,19]. The sections were compared with unstained ones [9], observed under polarized light, and examined under a light microscope. The streptavidin-biotin-complex/horseradish peroxidase approach was used in immunohistochemical procedures to identify the cellular composition of inflammatory infiltration (in certain circumstances) [20].

A semiobjective score system was used to characterize the amount of amorphous mineral deposits, with or without chondroid and osteoid or bone development (0-no mineral, chondroid etc. deposits, 1-minimal, 2-moderate, 3 abundant mineral deposition, chondroid, osteoid or bone formation. According to Bély M, et al. [9], conventionally stained tissue sections [17-19,21,22] were compared with unstained sections utilizing the Pearson's chi-squared ( $\chi^2$ ) test [23] (description of non-staining method see below).

Professional high-brightness (100-watt) light microscope (Olympus BX51) and polarized light were used to analyze standard and unstained tissue slices, respectively. In some cases, electron microscopy and electron

diffraction were also carried out using a JEM 100CX.

Using the student (Welch) t-probe, the demographics of Ch-C patients with different crystal deposits were compared [23]. The distinction between two patient cohorts was deemed "significant" at the 0.05 alpha level.

## Results

Prevalence of various crystals in clinically diagnosed chondrocalcinosis. Out of 40 tissue samples from 16 individuals with a clinical diagnosis of Ch-C, 11 (27.5%) had CPPD crystals in the HE stained tissue sections. HA, CC or CL crystals were not detected in HE stained tissue. Out of 40 samples, 22 (55.0%) had CPPD crystals in unstained tissue sections. These patients included all 16 who had a clinical diagnosis of Ch-C. Besides CPPD crystals, HA crystals were found in 26 tissue samples of all 16 patients, CC in 23 tissue samples of 12 patients, and CL in 11 tissue samples of 5 patients with clinically diagnosed Ch-C.

MSU crystals were not identified in these 16 patients with clinically diagnosed chondrocalcinosis. There were no discernible variations in the mean age of Ch-C patients with concurrent HA, CC, or CL crystals and those with CPPD crystals. More crystals of CPPD, HA, CC, and CL were found in unstained sections than in HE-stained ones (In HE stained tissue sections HA, CC and CL crystals were not find) (Table 1). The simultaneous CPPD, HA, CC, and CL crystals in 40 HE-stained and 40 unstained tissue samples from 16 patients with clinically confirmed Ch-C are summarized in Table 1.

Ch-C	HE stained Ts-Prevalence (in %)				Unstained Ts-Prevalence (in %)			
	CPPD	HA	CC	CL	CPPD	HA	CC	CL
<b>Patients n=16</b>	8 (50.0%) of 16	0 (0%) of 16	0 (0%) of 16	0 (0%) of 16	16 (100%) of 16	16 (100%) of 16	12 (75.0%) of 16	5 (31.25%) of 16
<b>Tissue samples n=40</b>	11 (27.5 %) of 40	0 (0%) of 40	0 (0%) of 40	0 (0%) of 40	22 (55%) of 40	26 (65 %) of 40	23 (57.5%) of 40	11 (27.5%) of 40

**Table 1:** Identified CPPD, HA, CC, and CL crystals in 40 HE stained and in 40 unstained tissue samples of 16 patients with clinically diagnosed Ch-C.

### Microscopic characteristics of CPPD (calcium pyrophosphate dihydrate [Ca<sub>2</sub>P<sub>2</sub>O<sub>7</sub>·2H<sub>2</sub>O]) crystal deposits in patients with clinically diagnosed chondrocalcinosis

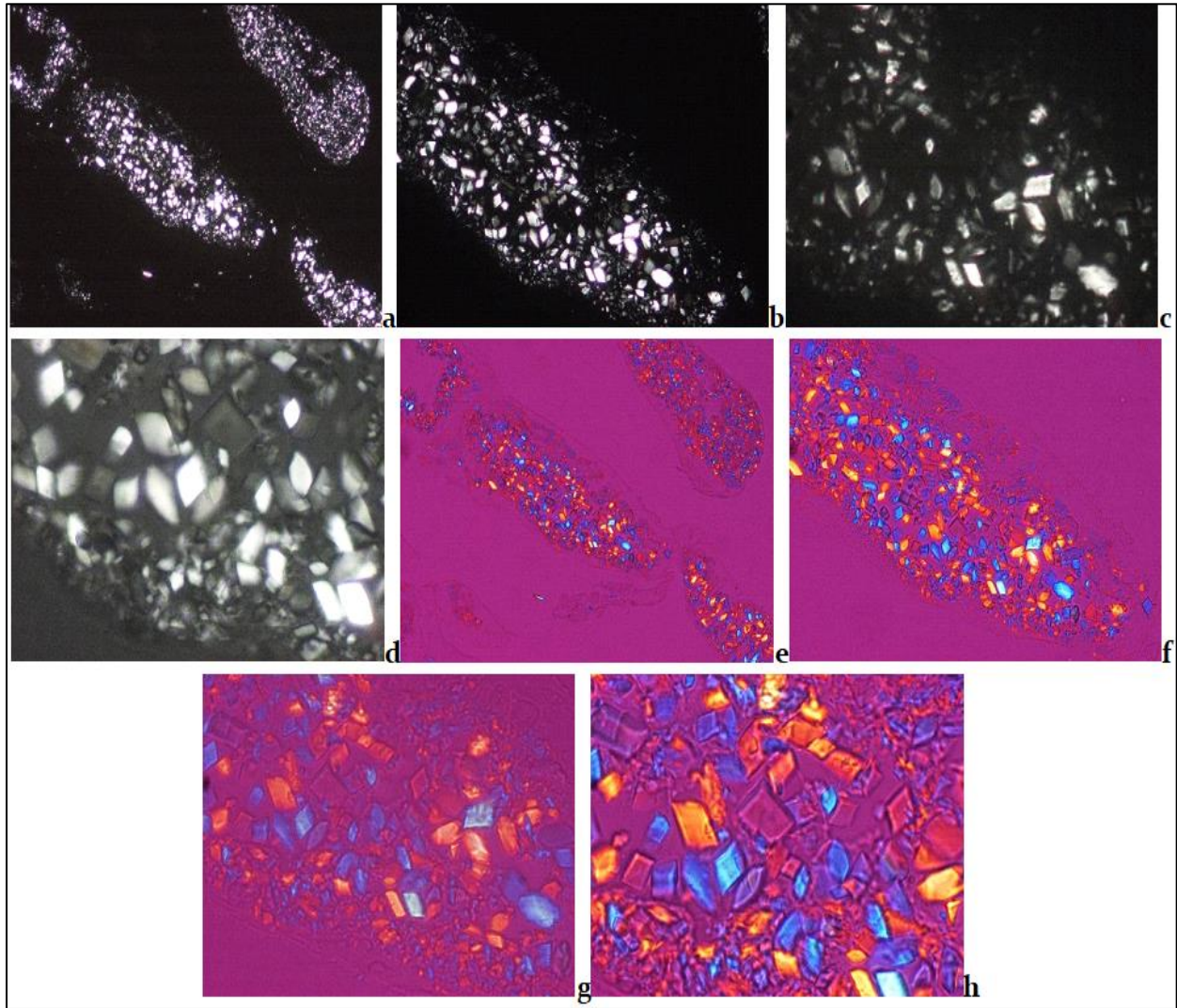
CPPD crystals appeared typically as planes of hexagonal, rhomboid, trapezoid, parallelogram-shape or fragments of these (Figures 1a-h). In contrast to the poor positive birefringence of HA crystals, the CPPD crystals displayed a rather strong positive birefringence when seen with polarized light using a Red I compensator (Figures 5a-h).

CPPD crystal deposition was accompanied with more or less amorphous calcium phosphate [Ca<sub>3</sub>(PO<sub>4</sub>)<sub>2</sub>] and/or calcium carbonate [CaCO<sub>3</sub>] deposits of irregular shape (Figure 2). Three tissue samples from a patient with Ch-C were not available for evaluation. Amorphous calcium phosphate [Ca<sub>3</sub>(PO<sub>4</sub>)<sub>2</sub>] and/or calcium carbonate [CaCO<sub>3</sub>] deposits were evaluated in 37 tissue sections of 15 patients in specimens stained with HE, Alizarin red S, or von Kossa reaction.

Based on the semi-objective score system in Ch-C patients the mineral deposition was 1.054 per tissue sections, representing a moderate calcification on a 0-3 semiobjective scale. In 2 patients the amorphous calcification was accompanied by minimal chondroid formation (0.054 per tissue sections); osteoid or newly formed bone tissue were not detected.

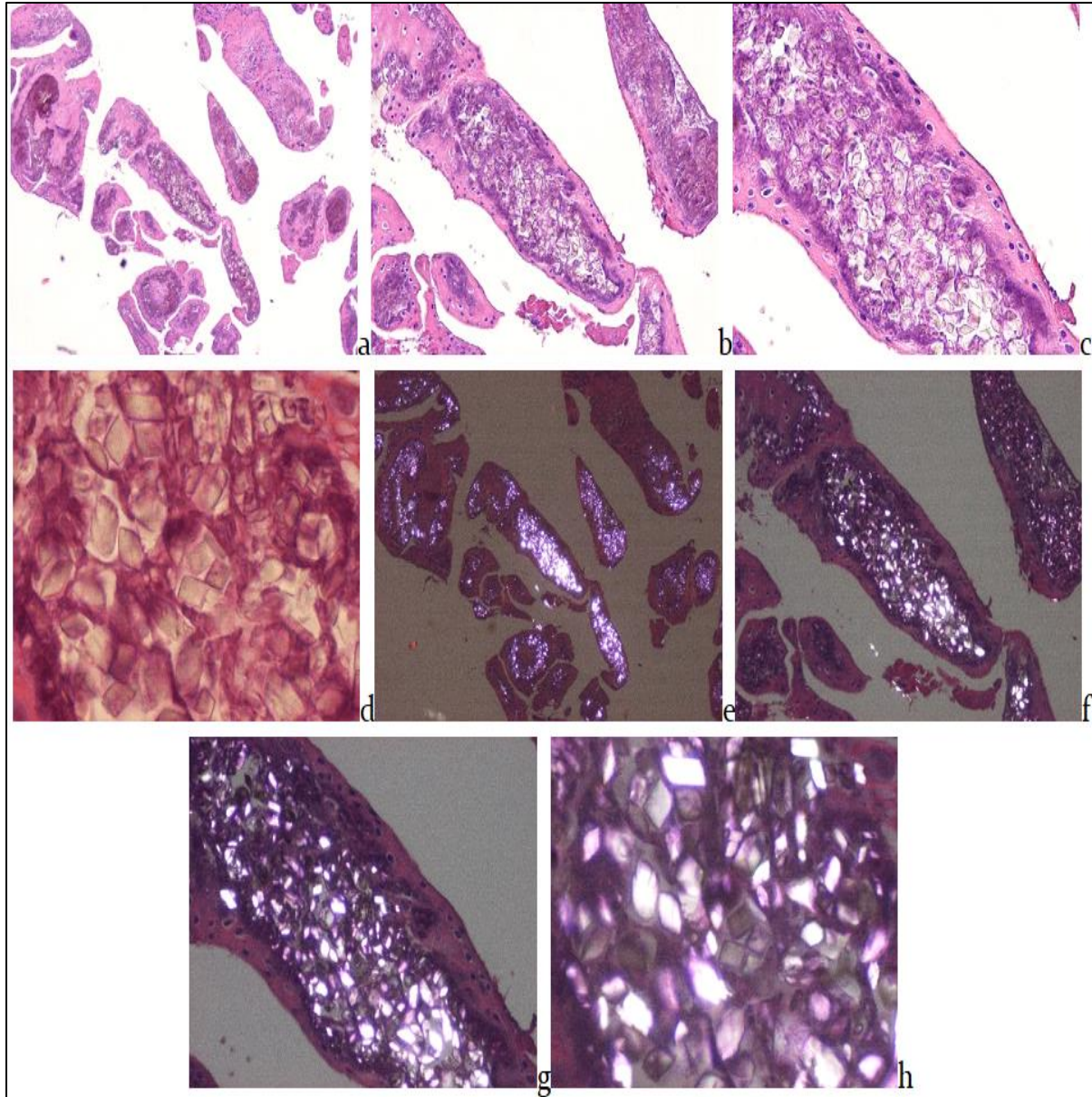
Occasionally the amorphous mineral deposits masked the CPPD crystals, but that remained intact and did not stain with Alizarin red S and did not react with von Kossa's reaction despite the calcium content in the crystalline structure (Figures 3 and 4).

Figure 1 demonstrates characteristic CPPD crystal deposits in a patient with clinically diagnosed chondrocalcinosis. The 24 × 36 mm transparent slide corresponds to the original magnifications of all light microscopic Figures; the right height:width ratio is 2:3. Since the printed size could differ, the original magnifications are displayed (Figure 1-11).



**Figure 1(a-h):** (Ch-C 437-86) Chondrocalcinosis, knee joint, synovial membrane, unstained section, viewed under polarized light without Red I compensator (a-d), and with Red I compensator (e-h). CPPD plane crystals are hexagonal, rhomboid, trapezoid, parallelogram-shape or fragments of these, that range in size from submicroscopic to 40 $\mu$ m, and show a relatively strong positive birefringence according to the long axis of the crystals with Red I compensator. (a) conventionally processed unstained tissue sections with CPPD crystals, viewed under polarized light at  $\times 100$ ; (b) identical to (a)  $\times 200$ ; (c) identical to (a)  $\times 400$ ; (d) identical to (a)  $\times 600$ ; (e) unstained sections with CPPD crystals, viewed under polarized light with a Red I compensator, identical to (a),  $\times 100$ ; (f) identical to (e)  $\times 200$ ; (g) identical to (f)  $\times 400$ , (h) identical to (g)  $\times 600$ .

Figure 2 demonstrates the amorphous calcium phosphate [ $\text{Ca}_3(\text{PO}_4)_2$ ], and/or calcium carbonate [ $\text{CaCO}_3$ ] deposits with HE stained tissue sections.



**Figure 2(a-h):** (Ch-C 437-86) Chondrocalcinosis, knee joint, synovial membrane, HE stained section, viewed with light microscope, and polarized light, respectively. Occasionally the amorphous mineral deposits mask the CPPD crystals. CPPD crystals are less soluble in aqueous dyes and may remain in conventionally processed surgical specimens stained by HE. (a) CPPD crystals, conventionally processed tissue sections, stained with HE, viewed with light microscope,  $\times 40$ , (c) same as (a)  $\times 100$ , (e) same as (a)  $\times 200$ , (g) same as (a)  $\times 600$  (b) CPPD crystals, conventionally processed unstained tissue sections, stained with HE, viewed under polarized light, same as (a),  $\times 40$ , (d) same as (c)  $\times 100$ , (f) same as (e)  $\times 200$ , (h) same as (g)  $\times 600$ .

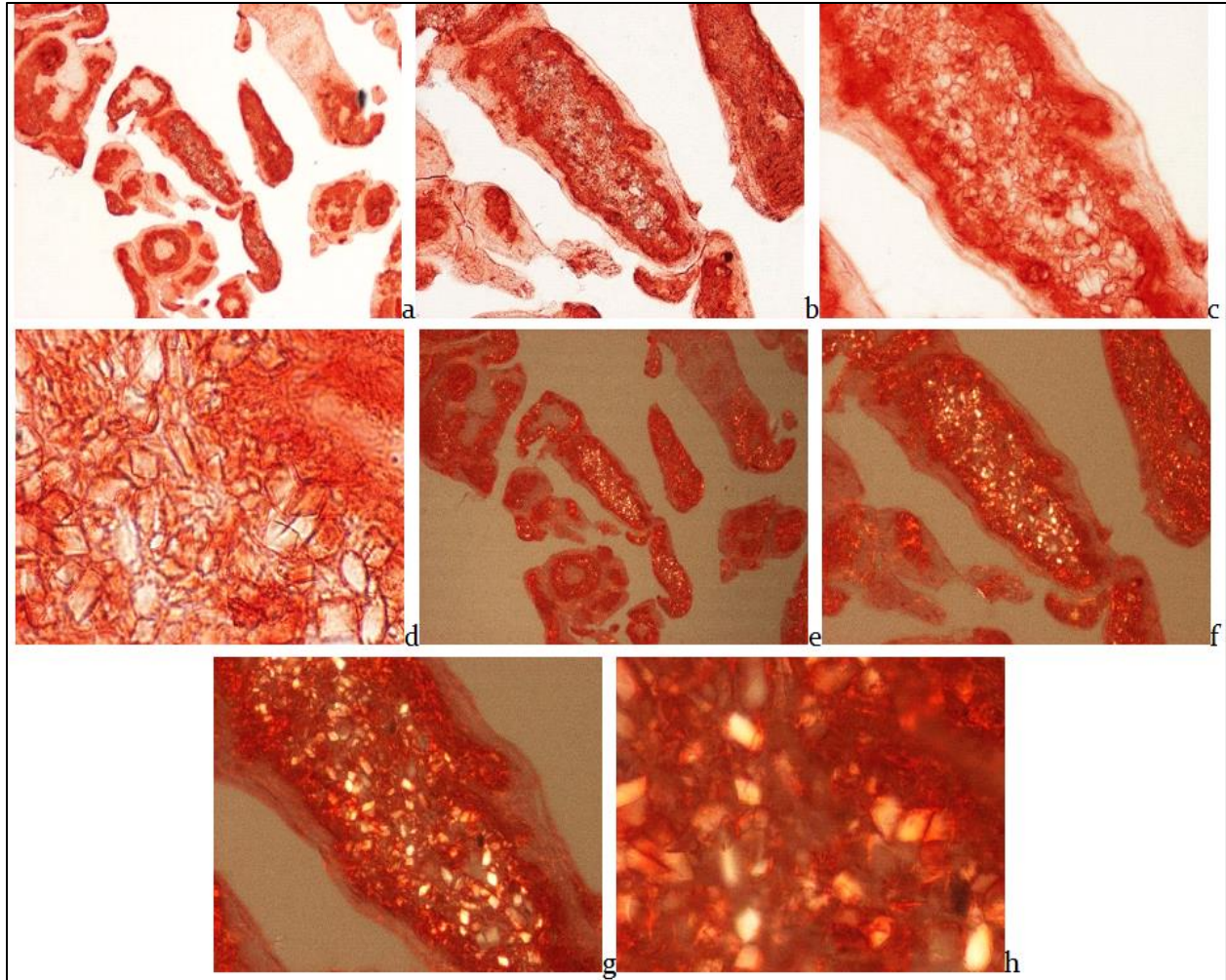


**Figure 3(a-h):** (Ch-C 437-86) Chondrocalcinosis, Alizarin red S staining (specific for calcium), viewed with the light microscope (a-d), and viewed with polarized light, respectively (e-h). The amorphous mineral deposits may mask the CPPD crystals, but despite the calcium content of the crystalline structure the crystals remain intact and do not stain with Alizarin red S. (a) Conventionally processed tissue samples, Alizarin red S staining, CPPD crystals and amorphous mineral deposit, unstained sections, viewed with light microscope,  $\times 40$ , (b) same as (a)  $\times 100$ , (c) same as (a)  $\times 200$ , (d) same as (a)  $\times 600$  (e) Tissue samples prepared conventionally, Alizarin red S staining, CPPD crystals, seen in polarized light, identical to (a),  $\times 40$ , (f) identical to (e)  $\times 100$ , and (g) identical to (f)  $\times 200$ , (h) same as (g)  $\times 600$ .

Figures 3 and 4 demonstrate amorphous calcium phosphate  $[\text{Ca}_3(\text{PO}_4)_2]$ , and/or calcium carbonate  $[\text{CaCO}_3]$  deposits with Alizarin red S staining (Figure 3), and with von Kossa reaction (Figure 4).

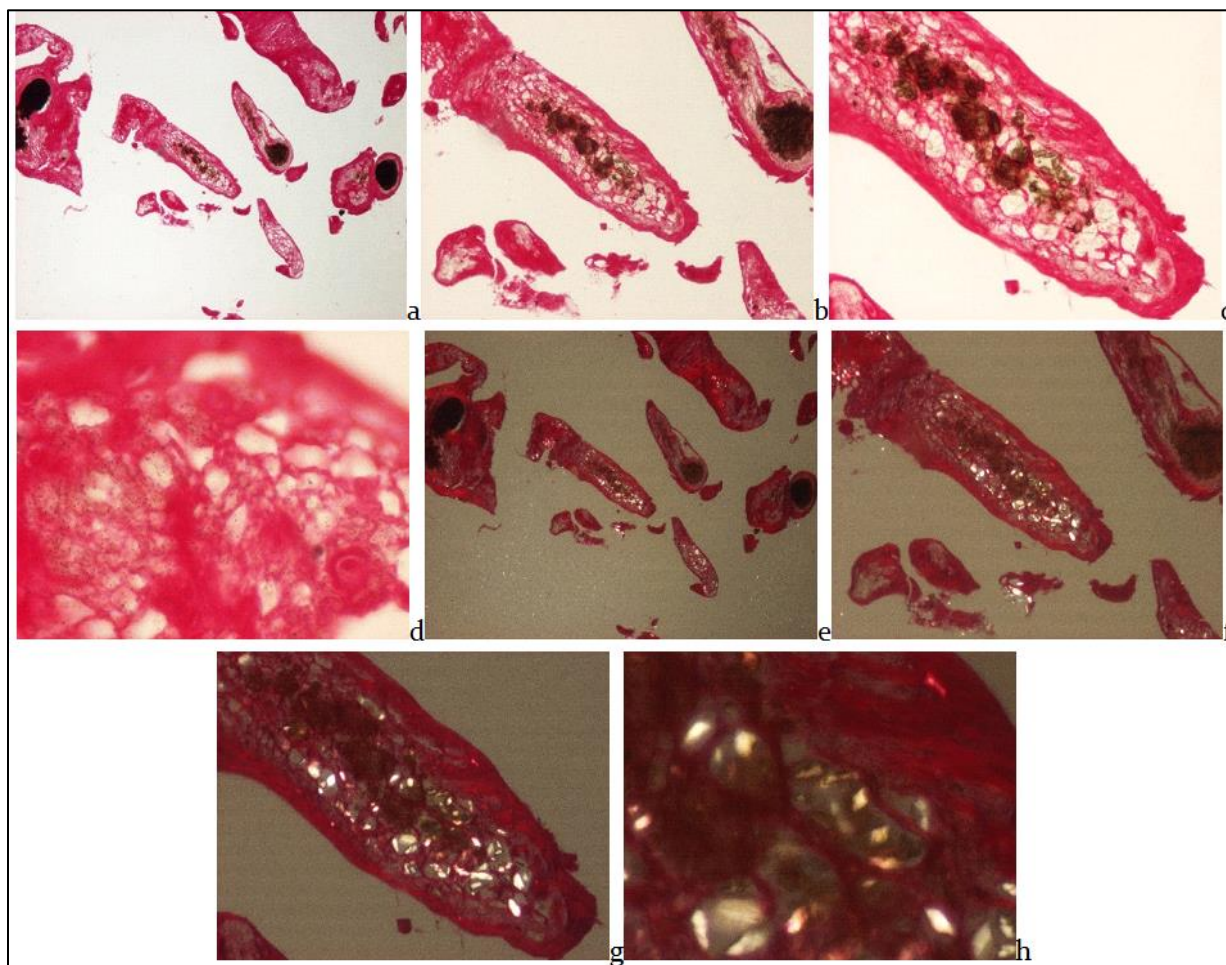


**Figure 4(a-h):** (Ch-C 437-86) Chondrocalcinosis, von Kossa reaction (specific for phosphatoo65 and/or carbonate), viewed with the light microscope (a-d), and viewed with polarized light (e-h). The amorphous mineral deposits may mask the CPPD crystals, but despite the calcium content the crystals remain intact and do not stain with the von Kossa reaction. (a) Conventionally processed tissue samples, von Kossa reaction, CPPD crystals and amorphous mineral deposits, viewed with light microscope,  $\times 40$ , (b) same as (a)  $\times 100$ , (c) same as (a)  $\times 200$ , (d) same as (a)  $\times 600$  (e) Conventionally processed tissue samples, von Kossa reaction, CPPD crystals, viewed under polarized light, same as (a),  $\times 40$ , (f) same as (e)  $\times 100$ , (g) same as (f)  $\times 200$ , (h) same as (g)  $\times 600$ .

### Microscopic characteristics of HA (hydroxyapatite [ $\text{Ca}_5(\text{PO}_4)_3(\text{OH})$ ]) crystal deposits in patients with clinically diagnosed chondrocalcinosis

In conventionally processed tissue section stained with HE, viewed with the light microscope HA crystals were not detected.

The individual HA crystals were tiny, colorless, or white, short to long rod-shaped prisms when observed in unstained sections under polarized light (Figure 5), hexagonal with bipyramidal or rounded endings electron microscopically (Figure 11c-d) or were arranged typically in 1-5  $\mu\text{m}$  spheroid microaggregates.



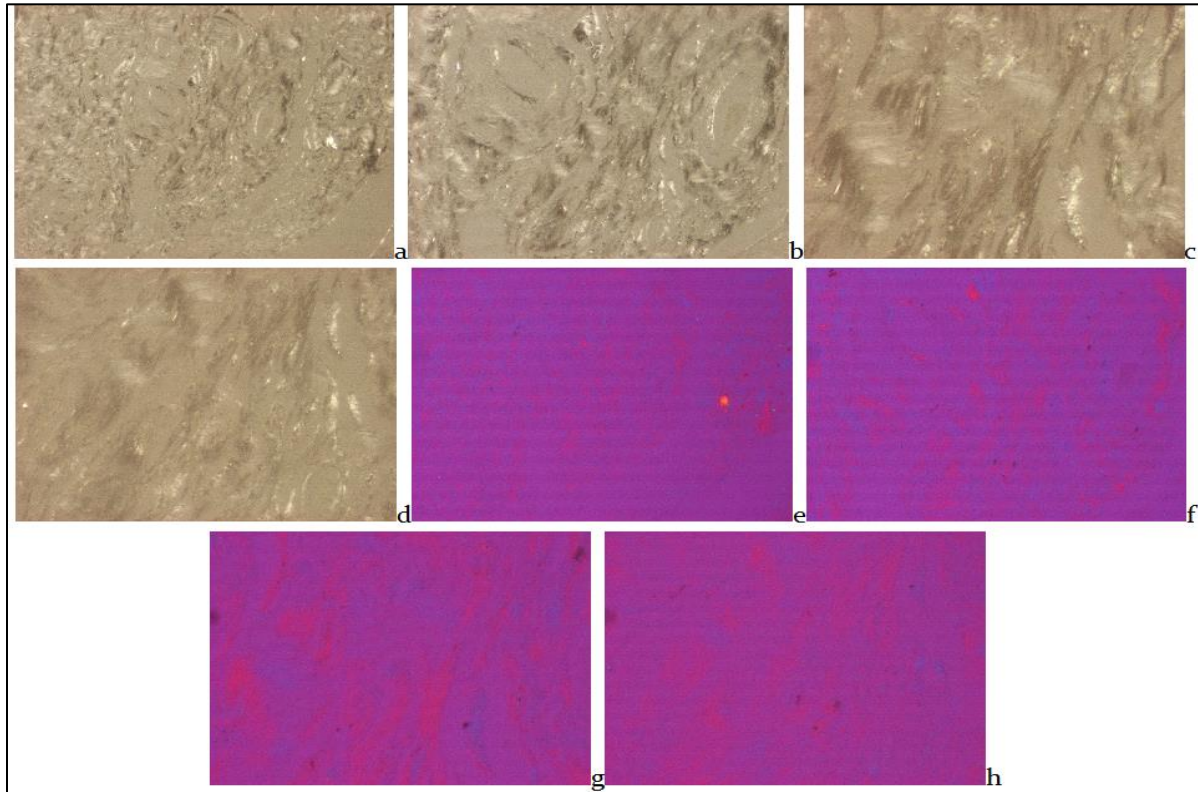


**Figure 5(a-h):** (Ch-C 2207-816) Chondrocalcinosis, knee joint, capsule, unstained section, viewed under polarized light without Red I compensator (a-d), and with Red I compensator (e-h). The birefringence of HA crystals is weak and positive, like that of the collagen fibers of the joint capsule. (a) Small prism of HA crystals between collaged fibers of joint capsule, conventionally processed tissue sections, observed in polarized light without the use of a Red I compensator  $\times 100$ , (b) identical to (a)  $\times 200$ , (c) identical to (a)  $\times 400$ , and (d) identical to (a)  $\times 600$  (e) Conventionally prepared unstained tissue sections with HA crystals seen under polarized light using a Red I compensator; (f) identical to (e)  $\times 40$ ; (g) identical to (f)  $\times 200$ ; and (h) identical to (g)  $\times 600$ .

Under polarized light using Red I compensator, the direction of birefringence was weak and positive according to the long axis of HA crystals, like that of collagen fibers (Figure 5). The CPPD crystals and the HA  $[\text{Ca}_5(\text{PO}_4)_3(\text{OH})]$  crystals were usually encircled by deposits of irregularly shaped calcium carbonate  $[\text{CaCO}_3]$  and/or more or less amorphous calcium phosphate  $[\text{Ca}_3(\text{PO}_4)_2]$  (see Figure 10 below, with dominant acute-subacute inflammatory infiltration). Figure 5 demonstrates

characteristic small prism of HA crystals with weak birefringence in a patient with clinically diagnosed chondrocalcinosis.

#### **Microscopic characteristics of CC (cholesterol $[\text{C}_{27}\text{H}_{46}\text{O}]$ ) crystals, and CL (crystalline liquid lipid) spherules in patients with clinically diagnosed chondrocalcinosis**

CC (with or without CL) were not detected in conventionally processed tissue section stained by HE.

In deparaffinized unstained tissue sections bizarre forms of cholesterol crystals were found, viewed with polarized light. The cholesterol crystals were present as rhomboidal notched separate plates (sheets) or needle-shaped clefts, typically arranged in clusters. Occasionally that was manifested as ovoid-biconvex or hexagonal bizarre forms and showed a transition between plate and globular lipid liquid form. A “semi-liquid” appearance of CC was also characteristic.

When CC or CL crystals were viewed under polarized light and with a Red I compensator, the birefringence was either positive or negative; needle-shaped or cleft crystal pieces revolving along the long axis, as well as rotated spherules, displayed positive or negative birefringence in the same place. Figures 6-8 demonstrate characteristics of cholesterol (Figures 6-7), semiliquid cholesterol, and crystalline liquid lipid droplets (Figure 8).

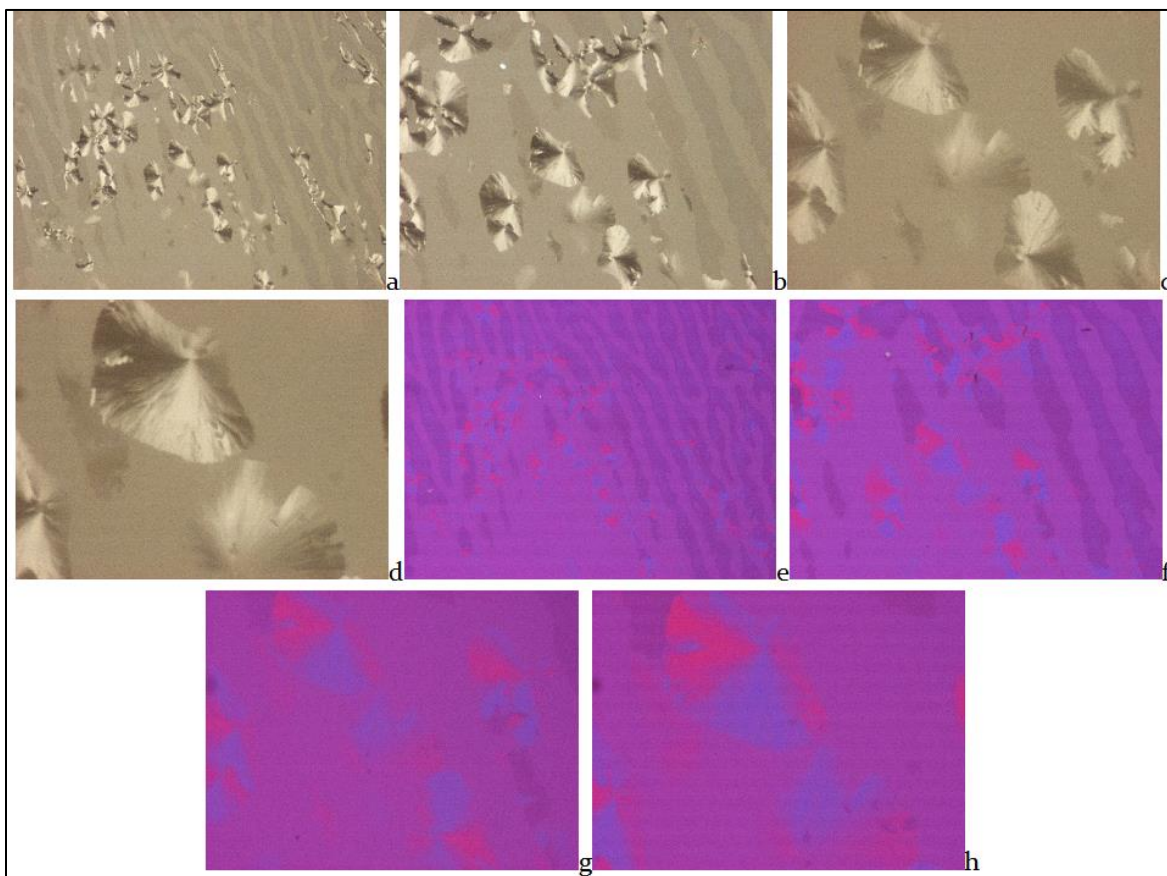


**Figure 6(a-h):** (Ch-C3558-2002) Chondrocalcinosis, synovial membrane, cholesterol crystals viewed under polarized light without Red I compensator (a-d), and with Red I compensator(e-h). This figure shows the unstained section of cholesterol crystals under polarized light without a Red I compensator ( $\times 100$ ), (b) the same as (a)  $\times 200$ , (c) the same as (a)  $\times 400$ , (d) the same as (a)  $\times 600$ , and (e) the same section of cholesterol crystals under polarized light with Red I compensator  $\times 100$ , same as (a), (f) the same as (e)  $\times 200$ , (g) the same as (f)  $\times 400$ , and (h) the same as (g)  $\times 600$ .

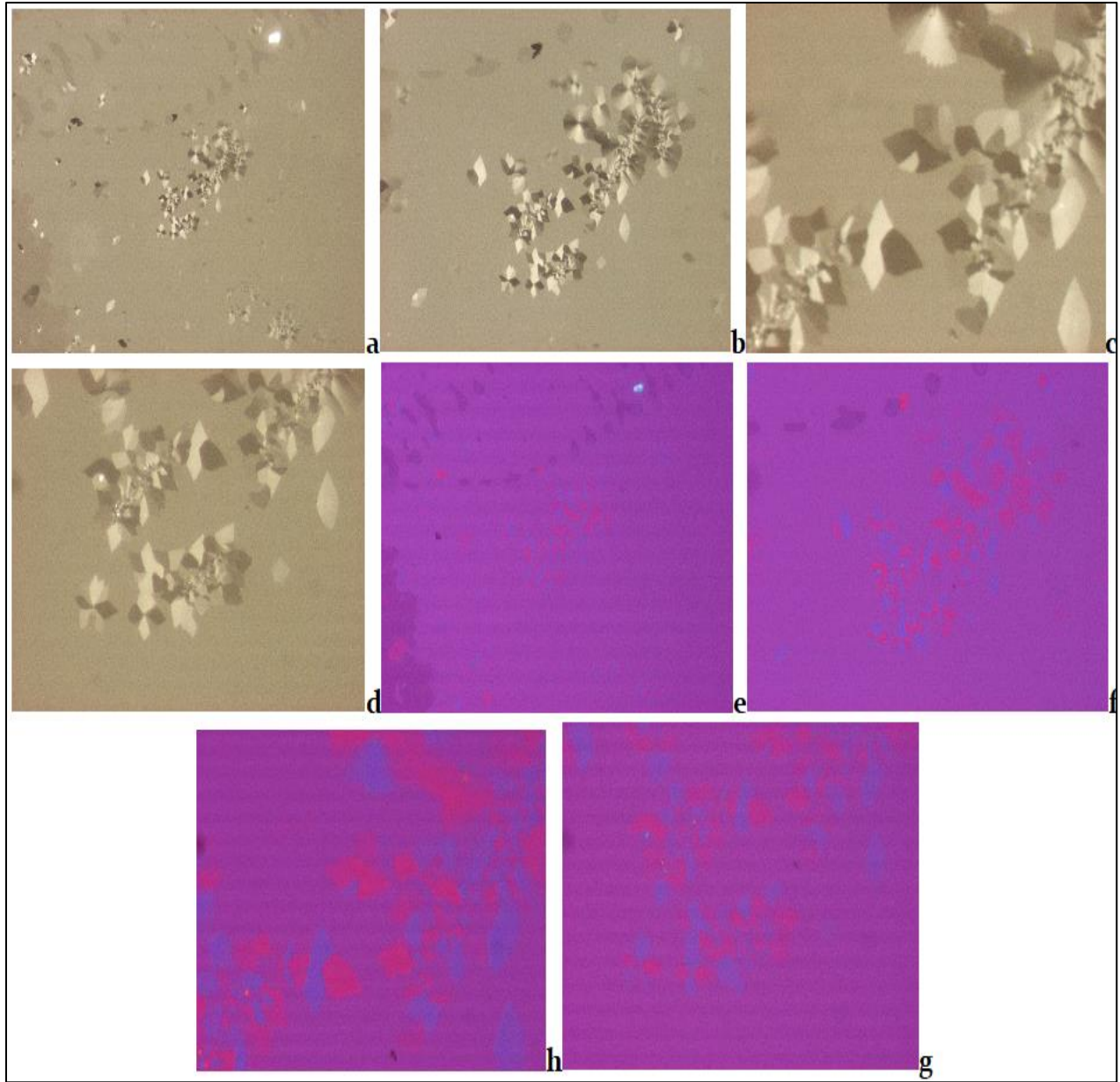


**Figure 7(a-h):** (Ch-C3558-2002) Chondrocalcinosis, synovial membrane, cholesterol crystals viewed under polarized light without Red I compensator (a-d), and with Red 1 compensator(e-h). (a)This figure shows the unstained section of cholesterol crystals under polarized light without a Red 1 compensator ( $\times 100$ ), (b) the same as (a)  $\times 200$ , (c) the same as (a)  $\times 400$ , (d) the same as (a)  $\times 600$ , and (e) the same section of cholesterol crystals under polarized light with Red 1 compensator ( $\times 100$ , same as (a)), (f) the same as (e)  $\times 200$ , (g) the same as (f)  $\times 400$ , and (h) the same as (g)  $\times 600$ .

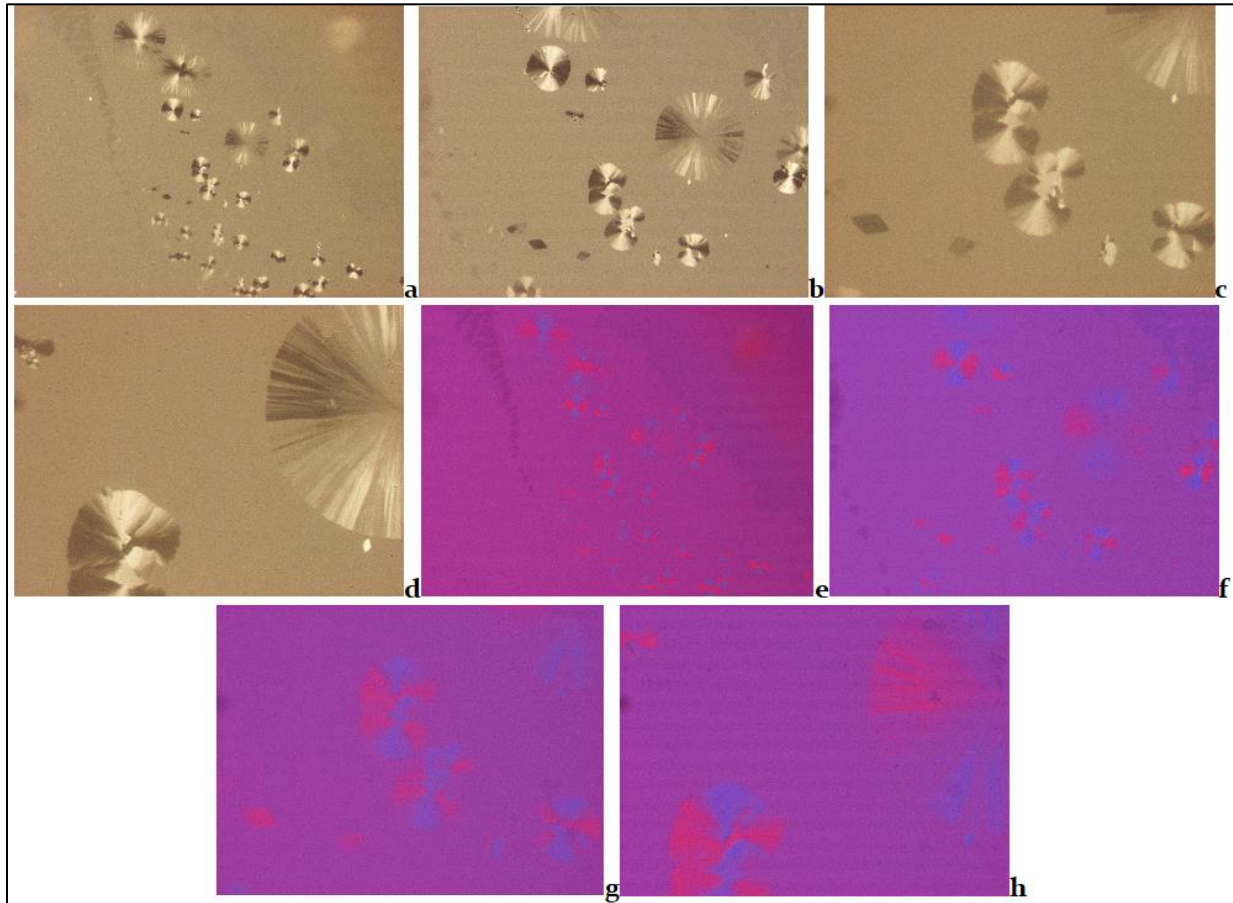


**Figure 8(a-h):** (Ch-C-2739-83) Chondrocalcinosis, joint capsule, crystalline lipid liquid spherules, viewed under polarized light without Red I compensator (a-d), and with Red 1 compensator(e-h). (a) Unstained portion of crystalline lipid liquid spherules observed under polarized light without the use of a Red 1 compensator,  $\times 100$ ; (b) identical to (a)  $\times 200$ ; (c) identical to (a)  $\times 400$ ; (d) identical to (a)  $\times 600$ ; (e) Crystalline lipid liquid spherules, unstained section, observed under polarized light using Red 1 compensator. The cholesterol crystal's birefringence in this figure is positive, similar to that of collagen fibers, at  $\times 100$ , same as (a), (f), same as (e),  $\times 200$ , g, same as (f),  $\times 400$ , and (h), same as (g),  $\times 600$ .

### Possible relationship between coexistent CPPD, HA, CC or CL crystals in tissue sections of patients with clinically diagnosed chondrocalcinosis

CPPD was detected in 22, HA in 26, with CC in 23, and CL in 11 of 40 unstained tissue sections (Table 1). CPPD (n=22) was associated with HA (n=26) in 20, with CC (n=23) in 16, and with CL in 9 of 40 unstained tissue sections. HA (n=26) was associated

with CC (n=23) in 16, and with CL in 10 of 40 unstained tissue sections. CC (n=23) was associated with CL in 10 of 40 unstained tissue sections. There was a significant and positive correlation between prevalence of CPPD and HA ( $c=0.9047$ ,  $\chi^2=12.0058$ ,  $p<0.0005$ ), and between prevalence of CPPD and CC ( $c=0.6146$ ,  $\chi^2=4.6387$ ,  $p<0.0312$ ).

The correlation was not significant, between prevalence of CPPD and CL ( $c=0.6941$ ,

$\chi^2=3.0410$ ,  $p<0.0811$ -NS). The links between HA and CC ( $c=0.2307$ ,  $\chi^2=0.4957$ ,  $p<0.4813$ -NS) or HA and CL were not significant ( $c=0.7808$ ,  $\chi^2=3.0438$ ,  $p<0.0810$ -NS). Between prevalence of CC and CL the correlation was

positive and significant ( $c=0.8497$ ,  $\chi^2=6.9299$ ,  $p<0.0084$ ). The statistical links (“p” values of significance) between coexistent CPPD, HA, CC and CL crystals in chondrocalcinosis are summarized in Table 2.

Chondrocalcinosis n=40 Ts	CPPD	HA	CC	CL
Coexistent crystal deposits	n=22 Ts	n=26 Ts	n=23 Ts	n=11 Ts
CPPD n=22 of 40 Ts		$c=0.9047$	$c=0.6146$	$c=0.6941$
		$\chi^2=12.0058$	$\chi^2=4.6387$	$\chi^2=3.0410$
		$p<0.0005$	$p<0.0312$	$p<0.0811$ -NS
HA n=26 of 40 Ts			$c=-0.2307$	$c=-0.7808$
			$\chi^2=-0.4957$	$\chi^2=-3.0438$
			$p<0.4813$ -NS	$p<0.0810$ -NS
CC n=23 of 40 Ts				$c=0.8497$
				$\chi^2=6.9299$
				$p<0.0084$

**Table 2:** Statistical links (“p” values of significance) of coexistent crystal deposits in chondrocalcinosis. HA-Calcium hydroxyapatite-[Ca<sub>5</sub>(PO<sub>4</sub>)<sub>3</sub>(OH)], CPPD-Calcium pyrophosphate dihydrate-[Ca<sub>2</sub>P<sub>2</sub>O<sub>7</sub>·2H<sub>2</sub>O], CC-Cholesterol crystals-[C<sub>27</sub>H<sub>46</sub>O], CL-Crystalline liquid lipid spherules, Ts-Tissue samples.

### Possible relationship between coexistent CPPD, HA, CC or CL crystals and inflammatory infiltration in tissue sections of patients with clinically diagnosed chondrocalcinosis

The CPPD crystal deposits in clinically diagnosed chondrocalcinosis with coexistent HA, CC or CL crystals were characterized by moderate subchronic-chronic inflammatory reaction of lympho-plasmacytes and macrophages (giant cells). Subchronic-chronic lympho-plasma cellular inflammatory infiltration and macrophages (giant cells) with or without phagocytosed crystals or fragments were found in 7 of 40 tissue sections of 16 patients with clinically

diagnosed Ch-C. In one of these 7 patients the inflammatory infiltration was more acute-subacute, with scattered lymphocytes and plasma cells; the CPPD and HA crystals were accompanied with minimal, focal amorphous calcification (Figure 10).

Subchronic-chronic inflammatory cellular infiltration was associated with CPPD in 4, with HA in 5, with CC in 6, and with CL in 4 of 40 tissue sections. Statistically there was no significant correlation between subchronic-chronic inflammation and CPPD ( $c=0.0526$ ,  $\chi^2=0.0857$ ,  $p<0.7697$ -NS), HA ( $c=0.1764$ ,  $\chi^2=0.0019$ ,  $p<0.9652$ -NS), CC ( $c=0.6991$ ,  $\chi^2=1.5416$ ,  $p<0.2143$ -NS) or CL ( $c=0.6640$ ,  $\chi^2=2.1544$ ,  $p<0.1421$ -NS).

Figures 9 and 10 demonstrate inflammatory infiltration associated with CPPD crystal deposits in a patient with clinically diagnosed chondrocalcinosis. Figures 9 demonstrates a

characteristic sub chronic-chronic lympho-plasma cellular infiltration with macrophages (giant cells) with phagocytosed CPPD and unidentified rod-shaped crystals.

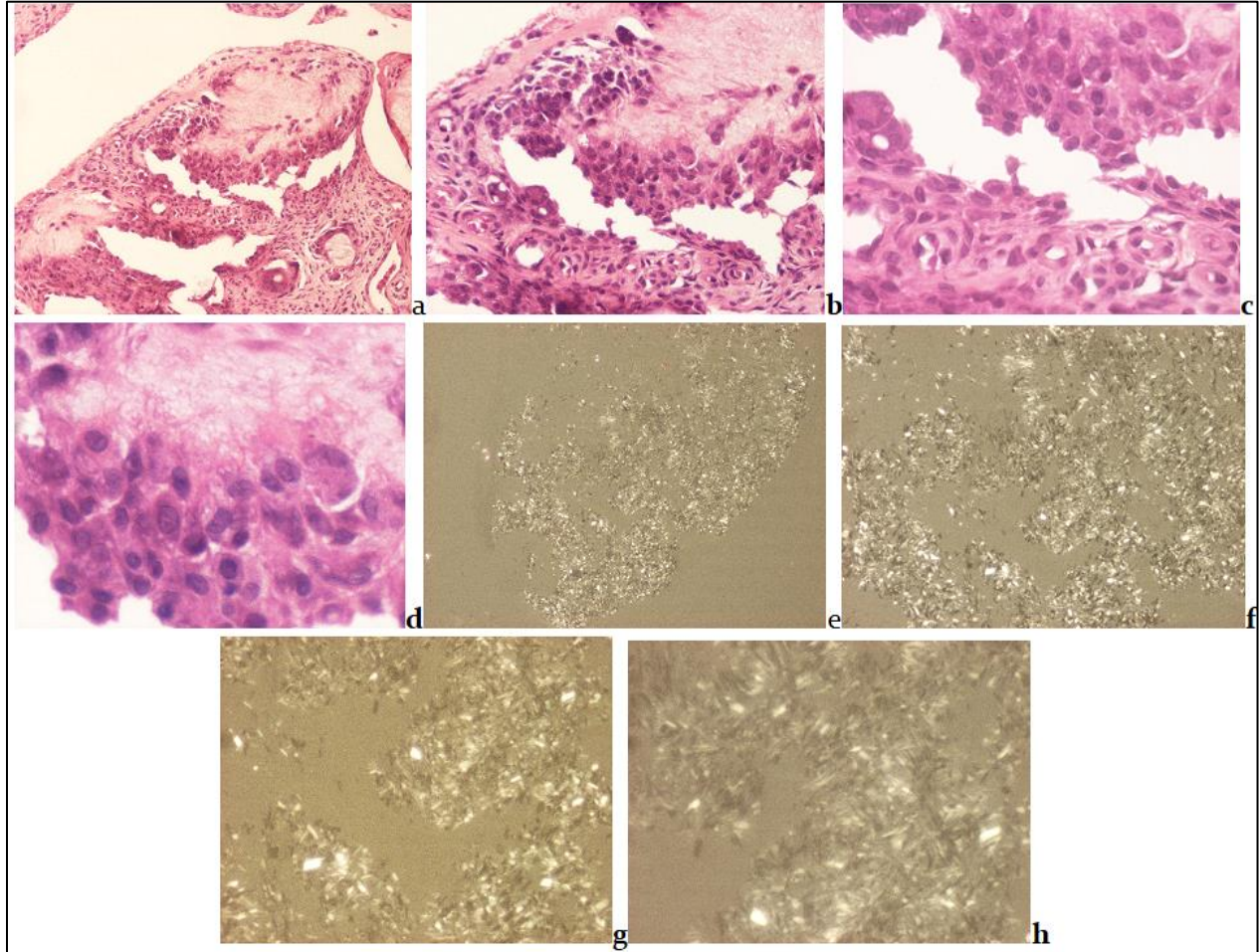


**Figure 9(a-h):** (Ch-C 581-2007) Chondrocalcinosis, knee, synovial membrane, sub chronic-chronic lympho-plasma cellular infiltration with macrophages (giant cells) with phagocytosed CPPD and unidentified rod-shaped crystals. (a) CPPD crystals, conventionally processed tissue samples stained with HE, viewed with the light microscope,  $\times 100$ , (b) same as (a)  $\times 200$ , (c) same as (a)  $\times 400$ , (d) same as (a)  $\times 600$  (e) CPPD crystals, conventionally processed unstained tissue sections, viewed under polarized light, same as (a),  $\times 100$ , (f) same as (e)  $\times 200$ , (g) same as (f)  $\times 400$ , (h) same as (g)  $\times 600$ .

Figures 10 demonstrates a dominant acute-subacute inflammatory infiltration with scattered lympho-plasma cellular infiltration in a patient with clinically diagnosed chondrocalcinosis. Viewed under polarized light the phagocytosed HA and fragmented CPPD crystals are demonstrated.

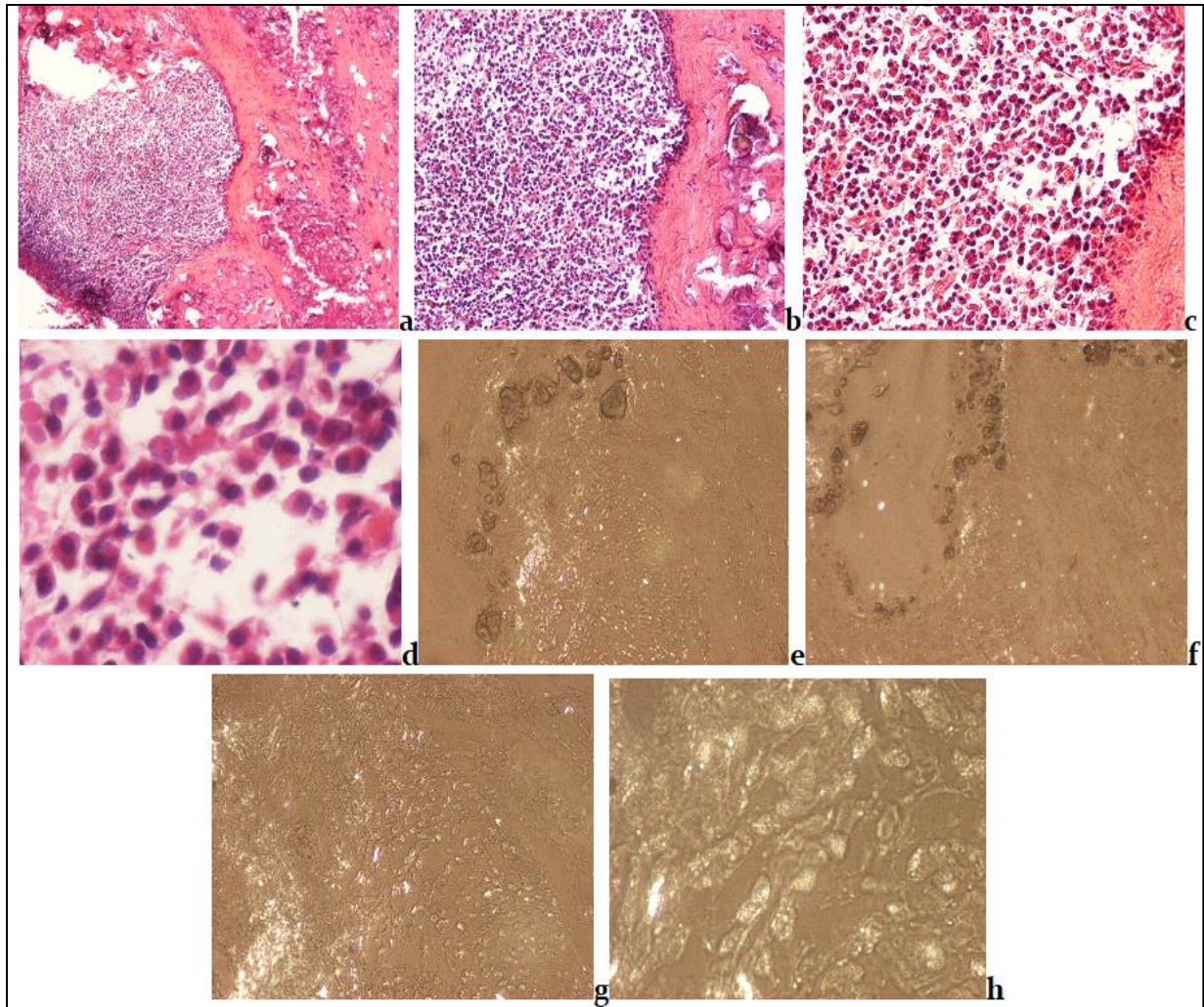


**Figure 10(a-h):** (Ch-C 676-81) Chondrocalcinosis, capsule of knee joint, acute-subacute cellular infiltration with lymphocytes and plasma cells. The inflammatory infiltration is accompanied with focal calcification, stained with HE, viewed with the light microscope (a-d), and viewed under polarized light (e-h). (a) Conventionally processed tissue section stained with HE,  $\times 40$ , (b) same as (a)  $\times 100$ , (c) same as (a)  $\times 200$ , (d) same as (a)  $\times 600$  (b), (e) Conventionally processed unstained tissues sections, phagocytosed HA crystals and CPPD fragments, viewed under polarized light,  $\times 40$ , (f) same as (e)  $\times 100$ , (g) same as (f)  $\times 200$ , (h) same as (g)  $\times 600$ .

Characteristic CPPD, HA and CC crystals are demonstrated by surface electron microscope in Figure 11.

The original electron microscopy Figure magnifications match the negative of  $60 \times 90$  mm.

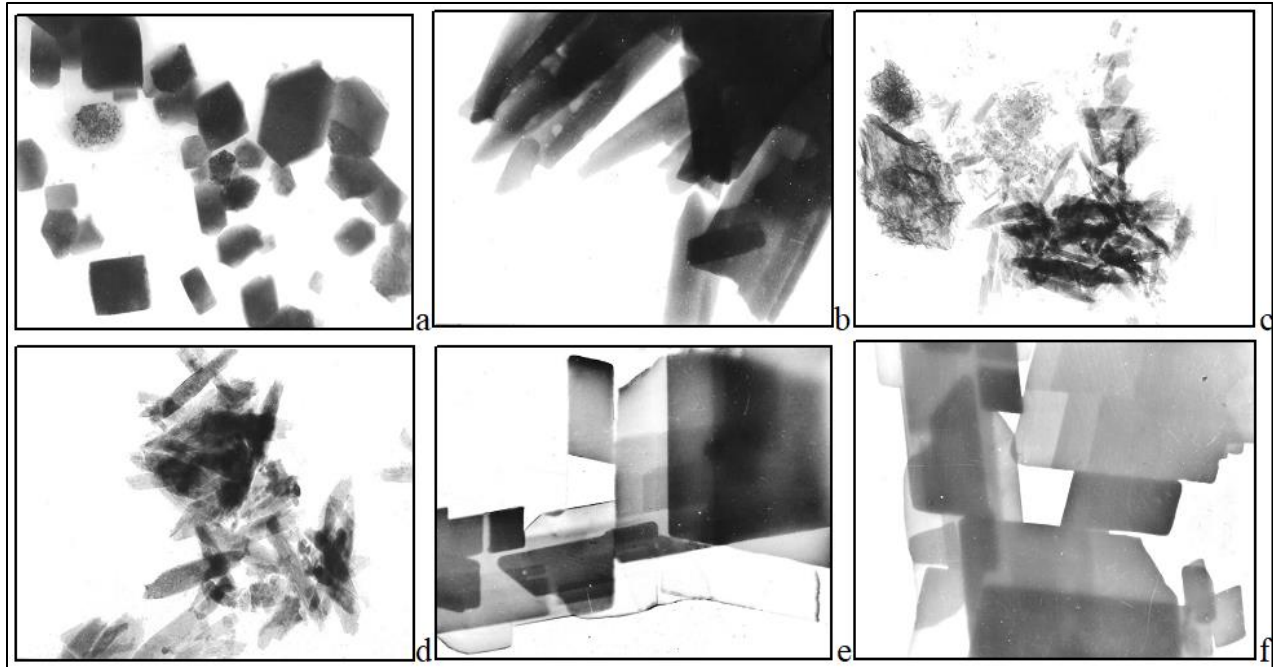


**Figure 11(a-f):** (CPPD 81/2020, 2726-80 and Cseresznyés HA 3495-97 26000x, 50000x, cholesterol 2734-83 × 1000, 2170-2019 × 1300)77. (a) Hexagonal-shaped plane crystals are CPPD crystals. parallelogram, trapezoid, rhomboid, or surface electron micrograph, × 10000, (b) CPPD crystals, rod-shape form, surface electron micrograph, × 10000 (c) Rod-shaped HA crystal cluster and small prisms, surface electron micrograph, × 20000, (d) surface electron micrograph of Rod-shaped HA crystals at × 50000, (e) Surface electron micrograph of cholesterol crystals at × 1300, (f) Surface electron micrograph of cholesterol crystals at × 1000 magnification.

## Discussion

### Ad 1

Compared to HA crystals, CPPD crystals are less soluble in an 8% aqueous formaldehyde solution or aqueous dyes; yet, on occasion, some CPPD crystals can be seen when polarized light is used to stain tissue slices with, HE, Alizarin red S, or the von Kossa reaction [14]. The non-staining approach is a practical, extremely easy, and more sensitive procedure for detection of CPPD, HA, CC or CL (furthermore other morphologically different and non-identified) crystals) in conventionally processed surgical specimens in comparison with the HE stained ones.

Comparing the mean ages of patients of chondrocalcinosis, containing CPPD, HA, CC or CL crystals separately, there was no significant difference between the groups. Concurrent HA, CC and/or CL associated with CPPD did not influence noteworthy the mean age of patient groups with clinically diagnosed chondrocalcinosis.

### Ad 2

In CPPD deposits the crystals typically are hexagonal, rhomboid, trapezoid, parallelogram-shape or are fragments of these (Figures 3a-h). While Gatter RA, et al. [26], state that the anticipated size range of CPPD is 0.42-17.9  $\mu\text{m}$  [25,26] it varies from



submicroscopic to 40  $\mu\text{m}$ . When viewed through a Red I compensatory with polarized light, the CPPD crystals exhibit a comparatively strong positive birefringence ( $\delta = 0.017$ ), whereas the HA crystals exhibit a modest positive birefringence ( $\delta = 0.007$ ).

CPPD crystals have modest and positive birefringence in contrast to the substantially negative birefringent MSU crystals. In the synovial membrane, menisci, or hyaline cartilage the deposited CPPD crystals are often asymptomatic. The CPPD crystals are generally surrounded by more or less amorphous mineral deposits, and the mineral deposits reduce the intensity of inflammation; the inflammatory response surrounding mineral deposits is typically either negligible or nonexistent.

Without mineral deposition, CPPD crystals can cause joint injury and a biological response, including the activation of macrophages. Affected joints typically experience extreme pain, swelling, and warmth [24]. In this study the calcium content of amorphous mineral deposits was detected by Alizarin red S staining in all 15 patients, and phosphate and/or carbonate deposits were identified by von Kossa reaction in 11 of 15 patients. The calcium and phosphate or carbonate deposition are presumably independent processes and are apparently distinct events of a mineral disorder.

### Ad 3

The individual HA crystals in synovial fluid [27] or in synovial membrane [28,29] can cause acute inflammation, and provoke

phagocytosis of neutrophilic leukocytes [30]. Acute inflammation may be accompanied with severe clinical symptoms: synovial fluid effusion, swelling, sudden onset of severe pain, tenderness, joint destruction of rapid progression, restricted motion, deformity, and instability of joints [31-33].

Individual HA crystals can range in size from submicroscopic to 1.9-15.6  $\mu\text{m}$  [8], according to Pay S, et al. [24], 50-500 nm or in clusters (“clumps”) 1-5  $\mu\text{m}$  [34]. HA crystals cannot be identified by conventional light microscopic techniques due to the small size or paucity. Furthermore, the majority of the clusters are less than 100 nm in diameter, i.e. below the visible range of light microscopy [25].

Clusters of HA crystals tend to form spherical clumps [5], and “can appear in HE stained tissue sections as shiny coins with traditional stains but show no birefringence under compensated polarized microscopy (400  $\times$ )” [31]. In unstained sections with a professional high-brightness (100-Watt) light microscope the HA crystal prisms and clumps can be well detected with polarized light and show positive birefringence using Red I compensator.

### Ad 4

The lipid complexes and cholesterol are still present in tissue slices that have been paraffin embedded and fixed in formaldehyde, even though the traditional processes involved the use of organic solvents such as xylene, methanol, terpene xylene, ethyl alcohol, and chloroform. When conventionally prepared tissue samples are studied under polarized light, a wide range of distinct forms of

cholesterol and lipid crystals can be observed without staining with aqueous dyes. Cholesterol and lipid complexes seem to be dissolved in HE or other aqueous dyes. There are methodological efforts to preserve the cholesterol and crystalline lipid droplets with different fixatives [21] or to transform the complexes into a non-soluble form resistant to aqueous dyes e.g. Schultz staining [22].

### Ad 5

The positive and significant correlation between CPPD and HA ( $p < 0.0005$ ) support the earlier premise that CPPD and HA represent basically an identical metabolic disorder) [14,25,35]. The positive link between CPPD and CC ( $p < 0.0312$ ) should be regarded an accidental coincidence in a relatively small patient population (in a larger patient population this relationship was not significant). The correlation between CPPD and CL ( $p < 0.0811$ ) was not significant. The correlations between HA and CC ( $p < 0.4813$ ) or HA and CL ( $p < 0.0810$ ) are not significant and suggest that the presence of CC (with or without CL) seems to be an independent fat metabolic malady.

### References

1. Dieppe PA, Crocker PR, Huskisson EC, Willoughby DA. Apatite Deposition Disease: A New Arthropathy. *Lancet*. 1976;307(7954):266-9. [PubMed](#) | [CrossRef](#)
2. Rosenthal AK, Ryan LM. Calcium Pyrophosphate Deposition Disease. *N Engl J Med*. 2016;374(26):2575-84. [PubMed](#) | [CrossRef](#)
3. Dieppe PA. Milwaukee Shoulder. *BBr Med J (Clin Res Ed)*. 1981;283(6305):1488. [PM](#). [PubMed](#) | [CrossRef](#)
4. Gardner DL, McClure J. Metabolic Nutritional and Endocrine Diseases of Connective Tissue, Crystal Deposition Disease, Calcium Pyrophosphate Dehydrate Crystal Deposition Disease (Chondrocalcinosis; Pseudogout). In: *Pathol Basis Connect Tissue Dis*. 1992:393-402.
5. Mohr W. "Calcium Pyrophosphate Arthropathy", "Apatite Diseases". In: Mohr W, editor. *Joint Pathol, Historical Foundations, Causes and Developments of Joint Diseases and their Pathomorphology*. Springer-Verlag Berl Heidelberg. 2000;193-201,201-212. [CrossRef](#)
6. Reginato AJ, Reginato AM. Diseases Associated with Deposition of Calcium Pyrophosphate or Hydroxyapatite. *Kelly's Textbook of Rheumatology*, ed. 2001;6:1377-90.

### Ad 6

The connection between inflammatory cellular infiltration and CPPD, HA, CC or CL crystals surrounded by mineral deposits was not significant.

### Conclusion

The nonstaining technique of Bély M, et al., is a much more effective method for the demonstration of crystals in metabolic diseases than reactions and conventional stains. The non-staining technique is a useful simple method for the detection of CPPD, HA, CC (with or without CL) and other crystals. CPPD and/or HA crystals can provoke inflammatory processes basically responsible for the clinical symptoms. The variable amounts of amorphous minerals enclose (isolate) the crystals, reducing or eliminating the inflammatory reaction. The authors assume that CC (with or without CL) is an associated phenomenon (concomitant fat metabolic malady) without direct cause of inflammation and is not responsible for clinical symptoms of crystal induced arthropathies.

7. Fassbender HG. Crystal-associated Arthropathies. *Pathol Pathobiol Rheum Dis.* 2002;353-79. [CrossRef](#)
8. Gupta SJ. Crystal Induced Arthritis: An Overview. *J Indian Rheumatol Assoc.* 2002;10:5-13.
9. Bély M, Apáthy Á. Mönckeberg's Sclerosis-crystal Induced Angiopathy. *Orv Hetil.* 2013;154(23):908-13. [CrossRef](#)
10. Bély M, Apáthy Á. Functional Role of Hydroxyapatite Crystals in Monckeberg's Arteriosclerosis. *J Cardiovasc Dis.* 2014;2:228-34.
11. Bély M, Apáthy Á. ABO<sub>843</sub> A Microscopic Method for Identification of Calcium Pyrophosphate Dihydrate Deposits in Tissues. *Ann Rheum Dis.* 2014;73(Suppl 2):1081.1-1081. [CrossRef](#)
12. Bély M, Apáthy Á. A Simple Method of Diagnostic Pathology for Identification of Crystal Deposits in Metabolic and Crystal Induced Diseases. *Struct Chem Crystallogr Commun.* 2016;2:1-5.
13. Bély M, Apáthy Á. Metabolic Diseases and Crystal Induced Arthropathies Technic of Non-staining Histologic Sections: A Comparative Study of Standard Stains and Histochemical Reactions. *Clin Arch Bone Joint Dis.* 2018;1(007). [CrossRef](#)
14. Bely BM. Crystal Deposits in Tissue of Patients with Chondrocalcinosis and Apatite Rheumatism-microscopic Identification of CPPD and HA with the Non-staining Technique of Bely and Apáthy. *BAOJ Clin Trials.* 2018;4:018.
15. Bély M, Krutsay M. A Simple Method to Demonstrate Urate Crystals in Formalin Fixed Tissue. *J Autoimmune Dis.* 2013;1(2):47. [CrossRef](#)
16. Carson FL. Mayer's Hematoxylin. *Histotechnology. A Selfinstructional Text.* 1990:100-4.
17. MacManus JF, Mowry RW, Harper and Row. Methods of General Utility for the Routine Study of Tissues. Sodium Alizarin Sulfonate Stain for Calcium and Von Kossa's Method for Phosphates and Carbonates. In: McManus JFA, Mowry RW, Staining Methods, Histologic and Histochemical. Hoeber PB Inc, New York. 1960:55-72.
18. Vacca LL. *Laboratory Manual of Histochemistry.* 1985.
19. Lillie RD. Von Kóssa's method. *Histopathologic Technic and Practical Histochemistry, The Blakiston Division McGraw-Hill Book Company, New York, Toronto, London, Editor: Lillie RD.* 1954:264-5.
20. Bratthauer GL. The Avidin-biotin Complex (ABC) Method and Other Avidin-biotin Binding Methods. *Methods Mol Biol.* 2010:257-70. [PubMed](#) | [CrossRef](#)
21. Pearse AG. Hexamine Silver Method for Uric Acid. *Histochemistry Theoretical and Applied, Churchill Livingstone, Edinburgh, London, Melbourne and New York, Editor: Pearse AGE.* 1985:1012-26.
22. Schultz A. On the Question of the Relationship between Leukemia and Gout: Also, Report on Histological Demonstration Methods of Uric Acid and Urates. *Virchows Arch Pathol Anat Physiol Klin Med.* 1931;280:519-29. [CrossRef](#)
23. Lentner C. Statistical Methods. Volume 2. In: Lentner C, Compiled by: Diem K, Seldrup J. *Geigy Scientific Tables.* Ciba-geigy Limited, Basle, Switzerland. 1982;227.
24. <https://www.mayoclinic.org/diseases-conditions/pseudogout/symptoms-causes/syc-20376983>
25. Swan A, Chapman B, Heap P, Seward H, Dieppe P. Submicroscopic Crystals in Osteoarthritic Synovial Fluids. *Ann Rheum Dis.* 1994;53(7):467-70. [PubMed](#) | [CrossRef](#)
26. Gatter RA, Schumacher HR. Microscopic Findings Under Compensated Polarised Light and Phase Light. *Practical Handbook of Joint Fluid Analysis.* 2nd ed. Philadelphia, London: Lea and Febiger. 1991:45-58.
27. Apáthy Á, Bély M. Crystal Induced Arthropathies-retrospective Analysis of Synovial Fluids Aspirated Between 2005 and 2017. *EC Cardiol.* 2022;9:15-31.
28. Bély M, Apáthy Á. Crystal Deposits in Apatite Rheumatism and Chondrocalcinosis-Microscopic Identification of Hydroxyapatite and Calcium Pyrophosphate Dihydrate Crystals with Standard Stains and Histochemical Reactions and with the Non-staining Technique of Bély and Apáthy. *EC Pulmonol Respir Med.* 2022;11:03-24.
29. Bély M, Apáthy Á. Apatite Rheumatism and Chondrocalcinosis are Different Stages of the Same Metabolic Disorder-A Clinicopathologic Study of 21 Patients with Clinically Diagnosed Apatite Rheumatism or Chondrocalcinosis. *J Interdiscip Histopathol.* 2022;10(8):1-14.
30. McCarty DJ. Crystals and Arthritis. *Dis Mon.* 1994;40(6):258-99. [PubMed](#) | [CrossRef](#)
31. Reginato AM, Yuvienco C. Hydroxyapatite Crystal-induced. *Rheumatology.* 2019.
32. Dieppe PA, Doherty M, Macfarlane DG, Hutton CW, Bradfield JW, Watt I. Apatite Associated Destructive Arthritis. *Rheumatology.* 1984;23(2):84-91. [PubMed](#) | [CrossRef](#)

Bély M | Volume 2; Issue 1 (2024) | Mapsci-JOCR-2(1)-014 | Research Article

**Citation:** Apáthy A, Bély M. CPPD and Associated Crystals in Clinically Diagnosed Chondrocalcinosis: A Clinicopathological Study of 20 Patients. *J Orth Clin Res.* 2024;2(1):122-41.

**DOI:** [https://doi.org/10.37191/Mapsci-JOCR-2\(1\)-014](https://doi.org/10.37191/Mapsci-JOCR-2(1)-014)

33. Bachmann D, Resnick D. Calcium Pyrophosphate Dihydrate Crystal Deposition Disease and Calcium Hydroxyapatite Crystal Deposition Disease. In: Bachmann D, Resnick D, editors. Radiological Atlas of Rheumatological Diseases. Editions Roche, F. Hoffmann-La Roche Ltd., Basel, Switzerland. 1994;108-116:117-123.
34. Pay S, Terkeltaub R. Calcium Pyrophosphate Dihydrate and Hydroxyapatite Crystal Deposition in the Joint: New Developments Relevant to the Clinician. *Curr Rheumatol Rep.* 2003;5(3):235-243. [PubMed](#) | [CrossRef](#)
35. Bély M, Apáthy A. ABo82o Calcium Pyrophosphate Dihydrate and Hydroxyapatite Crystal Induced Metabolic Diseases-same or Different? 2016;75:1184. [CrossRef](#)

## Appendix

Bély and Apáthy's "non-staining" technique [9-15].

- 8% neutral buffered formalin (at pH 7.6 for more than 24 hours at 20 Co room temperature) is used to fix tissue blocks of surgically removed specimens.
- Sections of 5 µm are cut from tissue blocks that have been dried in ethyl alcohol and embedded in paraffin using acetone and xylene.
- Extended deparaffinization in a thermostat set to 56°C for three to five days (with daily xylene changes).
- In solution of Chloroform-methanol I (1:1) for 1 hour.
- And then in solution of Chloroform-methanol II (1:1) for 1 hour or overnight.
- Using terpene xylene and xylene, mounting in Canada balsam, cover slip, and dehydration in ethyl alcohol (two changes of 96% alcohol I-II 30-30 min).

## Results

The abundance of CPPD and MSU crystals is higher in deparaffinized tissue sections of formaldehyde fixed and paraffin embedded surgical specimens without staining with aqueous dyes than in sections stained with HE or with other staining methods. In unstained sections the HA crystals, furthermore the cholesterol crystals and crystalline lipids are preserved, and are well detectable with polarized light (in HE stained sections the HA crystals or CC and CL cannot be detected).